THE COMPANY OF
Biologists

RESEARCH ARTICLE

Nephric duct insertion requires EphA4/EphA7 signaling from the pericloacal mesenchyme

Anna-Carina Weiss[1], Rannar Airik[1], Tobias Bohnenpoll[1], Franziska Greulich[1], Anna Foik[1], Mark-Oliver Trowe[1], Carsten Rudat[1], Frank Costantini[2], Ralf H. Adams[3] and Andreas Kispert[1,*]

ABSTRACT

The vesico-ureteric junction (VUJ) forms through a complex developmental program that connects the primordium of the upper urinary tract [the nephric duct (ND)] with that of the lower urinary tract (the cloaca). The signals that orchestrate the various tissue interactions in this program are poorly understood. Here, we show that two members of the EphA subfamily of receptor tyrosine kinases, EphA4 and EphA7, are specifically expressed in the mesenchyme surrounding the caudal ND and the cloaca, and that $Epha4^{-/-}$; $Epha7^{+/-}$ and $Epha4^{-/-};Epha7^{-/-}$ (DKO) mice display distal ureter malformations including ureterocele, blind and ectopically ending ureters with associated hydroureter, megaureter and hydronephrosis. We trace these defects to a late or absent fusion of the ND with the cloaca. In DKO embryos, the ND extends normally and approaches the cloaca but the tip subsequently looses its integrity. Expression of $Gata3$ and $Lhx1$ and their downstream target Ret is severely reduced in the caudal ND. Conditional deletion of ephrin B2 from the ND largely phenocopies these changes, suggesting that EphA4/EphA7 from the pericloacal mesenchyme signal via ephrin B2 to mediate ND insertion. Disturbed activity of this signaling module may entail defects of the VUJ, which are frequent in the spectrum of congenital anomalies of the kidney and the urinary tract (CAKUT) in human newborns.

KEY WORDS: CAKUT, Eph, Ephrin, Nephric duct, Vesicoureteric junction obstruction, Mouse

INTRODUCTION

Congenital anomalies of the kidney and urinary tract (CAKUT) are amongst the most common human birth defects. They comprise a wide range of structural and functional malformations of the individual components of the urinary system as well as their interfaces. A prominent subclass of CAKUT is characterized by improper ureter-bladder connectivity including distal ureters that end blindly, ectopically or form a ureterocele, which is a fluid-filled sac in or at the bladder. These vesico-ureteric junction (VUJ) anomalies obstruct urinary drainage into the bladder and result in dilation of the ureter (hydro- or megaureter) and renal pelvis (hydronephrosis), a disease entity that may culminate in destruction of the renal parenchyma (Nakai et al., 2003; Kerecuk et al., 2008; NAPRTCS, 2007).

[1]Institut für Molekularbiologie, Medizinische Hochschule Hannover, D-30625 Hannover, Germany. [2]Department of Genetics and Development, Columbia University Medical Center, New York, NY 10032, USA. [3]Max-Planck-Institute for Molecular Biomedicine, Department of Tissue Morphogenesis, and University of Münster, Faculty of Medicine, D-48149 Münster, Germany.

*Author for correspondence (kispert.andreas@mh-hannover.de)

Formation of a patent VUJ is the result of a complex morphogenetic program that connects the primordium of the upper urinary tract [the nephric duct (ND)] with that of the lower urinary tract (the cloaca) during embryonic development. The ND is an epithelial tube that in the mouse forms around embryonic day (E) 8.0 at the level of the forelimb buds and subsequently extends posteriorly within the intermediate mesoderm. At ~E9.75, the ND turns towards the midline and inserts into the cloaca that arises as an endodermal infolding. At E10.5, an epithelial diverticulum called the ureteric bud (UB) evaginates from the ND at the level of the hindlimb buds and invades the surrounding mesenchyme termed the metanephric blastema. The tip of the UB subsequently engages in repetitive rounds of elongation and branching and ultimately generates the collecting duct system of the kidney. The stalk region merely elongates to form the epithelial component of the ureter. From E12.5 onwards, the distal end of the stalk separates from the ND and integrates into the developing bladder wall. This process depends on the apoptotic removal of the common nephric duct (CND), which is the most caudal segment of the ND, and the subsequent growth of the bladder to move the ureter orifice to its final position. The epithelial lining of the collecting duct system, of the ureter and of the bladder subsequently differentiates into the urothelium, and the surrounding mesenchyme of these organs differentiates into layers of smooth muscle (SM) cells. Thus, the functional architecture of the urinary drainage system is established at ~E16.5 (Airik and Kispert, 2007; Uetani and Bouchard, 2009; Woolf and Davies, 2013).

Although the molecular and cellular causes of human VUJ anomalies have remained poorly understood (Weber, 2012), mutational analyses in the mouse have identified a number of crucial factors and steps for the proper integration of the distal ureter into the bladder (Mendelsohn, 2009; Uetani and Bouchard, 2009). Analysis of mice deficient for the transcription factor gene $Gata3$, the retinoic acid (RA) synthesizing gene $Aldh1a2$ and the gene encoding the receptor tyrosine kinase Ret revealed that a delay or a failure of ND insertion into the cloaca can cause ectopic ureters that join the bladder abnormally or remain fused to the ND. RA signaling and Gata3 independently regulate Ret expression in the ND, which in turn seems to be required for the formation of cellular protrusions that guide the posterior extension of the tube (Chia et al., 2011). Ret signaling is also crucial in UB formation and subsequent branching morphogenesis (Costantini and Shakya, 2006). Mispositioning of the UB by altered expression of the Ret ligand $Gdnf$ or perturbed downstream signaling dramatically affects how the ureter will join the bladder. UBs emerging posterior to the normal sprouting site will insert in the primitive bladder prematurely, which can lead to ectopically positioned distal ureters and, hence, vesico-ureteric reflux. Ureters emerging at an abnormally anterior site remain attached either to the ND, the urethra or to the bladder neck, leading to VUJ obstruction (Mackie and Stephens, 1975; Uetani and Bouchard, 2009). Hydro- or

DEVELOPMENT

megaureter and ureterocele are also observed as a consequence of a deficit in distal ureter maturation. This process depends on apoptotic removal of the CND, which is triggered by paracrine RA signaling and mediated by protein phosphatases Ptprs and Ptprf, which antagonize Ret signaling in the CND (Batourina et al., 2002, 2005; Uetani et al., 2009).

Eph/ephrin signaling is crucial both in development and tissue homeostasis (for recent reviews see Klein, 2012; Pitulescu and Adams, 2010). It affects cell behavior largely by modifying the cytoskeleton and conferring adhesive or repulsive properties to mediate cell positioning and segregation, oriented cell migration and tissue boundary formation. Eph receptors are subdivided into the EphA family with ten members and the EphB family with six members. EphA and EphB receptors preferentially interact with the six glycosylphosphatidylinositol-linked ephrin A ligands and the three transmembrane ephrin B ligands, respectively. Eph/ephrin signaling can act bi-directionally, with intracellular pathways operating downstream of both the Eph receptor (forward signaling) and the ephrin ligand (reverse signaling) (Kullander and Klein, 2002).

Reports on a role of Eph/ephrin signaling in urinary tract development have remained scarce. EphB2/ephrin B1 signaling has been implicated in regulation of the cytoarchitecture of medullary tubule cells (Ogawa et al., 2006) and reverse signaling mediated by ephrin B2 and EphB2 in the orchestration of urorectal septation (Dravis et al., 2004). Here, we provide evidence that Eph/ephrin signaling also plays a crucial role in establishing ureter-bladder connectivity.

RESULTS
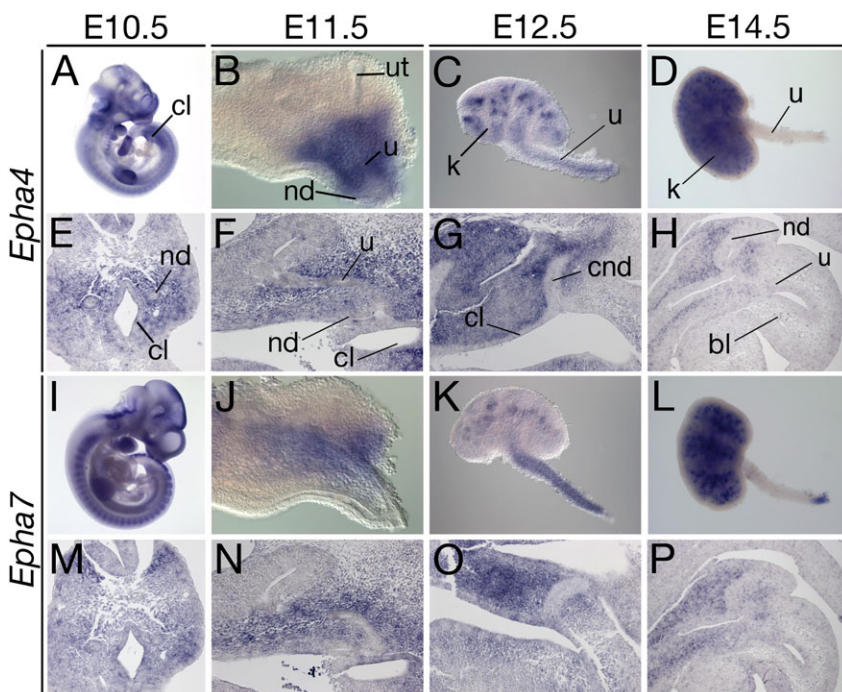### *Epha4* and *Epha7* expression during urinary system development
We have recently shown that the T-box transcription factor gene *Tbx18* plays an important role in the specification of the ureteric mesenchyme (Airik et al., 2006; Bohnenpoll et al., 2013). To identify downstream mediators of Tbx18 function in this tissue, we compared the transcriptional profile of wild-type and *Tbx18*-deficient ureters of E13.5 embryos by a preliminary microarray analysis. Among the genes with at least 2-fold downregulation in the mutant ureter, we

identified one member of the Eph receptor family, *Epha7*. Subsequent RNA *in situ* hybridization analysis of all known genes encoding Eph receptors on E12.5 ureters revealed coexpression of *Epha7* and *Epha4* with *Tbx18* in the ureteric mesenchyme (data not shown).

To obtain a detailed profile of *Epha4* and *Epha7* expression in ureter development, we performed whole-mount and section *in situ* hybridization analyses of E10.5 to E14.5 embryos and kidney rudiments. At E10.5, *Epha4* mRNA was found in the urogenital ridge and in mesenchyme surrounding the cloaca and the ND. Expression in this domain was maintained at E11.5 and E12.5, then encompassing the mesenchyme surrounding the primitive bladder, the ND and (more weakly) the ureter. At E12.5, additional expression of *Epha4* was detected in the metanephros (analysis to be reported in more detail elsewhere). At E14.5, *Epha4* expression in the ureteric mesenchyme was abolished, whereas expression around the distal ND and the urethra as well as renal expression persisted (Fig. 1A-H). *Epha7* was co-expressed with *Epha4* in the mesenchyme surrounding the cloaca/bladder, the distal ND and the ureter at all analyzed stages (Fig. 1I-P). Expression of *Epha4* and *Epha7* was maintained in the pericloacal mesenchyme of *Tbx18*-deficient embryos at E11.5 and E12.5, whereas expression of both genes was lost in the mutant ureteric mesenchyme at E12.5 (supplementary material Fig. S1), arguing for a *Tbx18*-independent function in the pericloacal mesenchyme and a *Tbx18*-dependent role in the ureteric mesenchyme during development of the urinary tract.

Combined deletion of *Epha4* and *Epha7* results in severe hydro/megaureter and hydronephrosis
To investigate the functional requirement of EphA4 and EphA7 in urinary tract development, we analyzed mice mutant for previously described null alleles of *Epha4* (Kullander et al., 2001) or *Epha7* (Dufour et al., 2003) for morphological changes in the urogenital system at E18.5. Mice single homozygous for either *Epha4* (*n*=8) or *Epha7* (*n*=33) featured a urogenital system that was indistinguishable from that of the wild-type control at this stage (Fig. 2A-C). By contrast, both $Epha4^{-/-};Epha7^{-/-}$ (DKO) as well as $Epha4^{-/-};Epha7^{+/-}$ urogenital systems displayed a severe

Fig. 1. Expression of *Epha4* and *Epha7* during ureter development. RNA *in situ* hybridization analysis on whole embryos (A,I), on kidneys with ureters (B-D,J-L), and on transverse (E,M) and sagittal (F-H,N-P) sections through the posterior trunk region for expression of *Epha4* and *Epha7* in wild-type mouse embryos from E10.5 to E14.5. bl, bladder; cl, cloaca; cnd, common nephric duct; k, kidney; nd, nephric duct; u, ureter; ut, ureter tip.
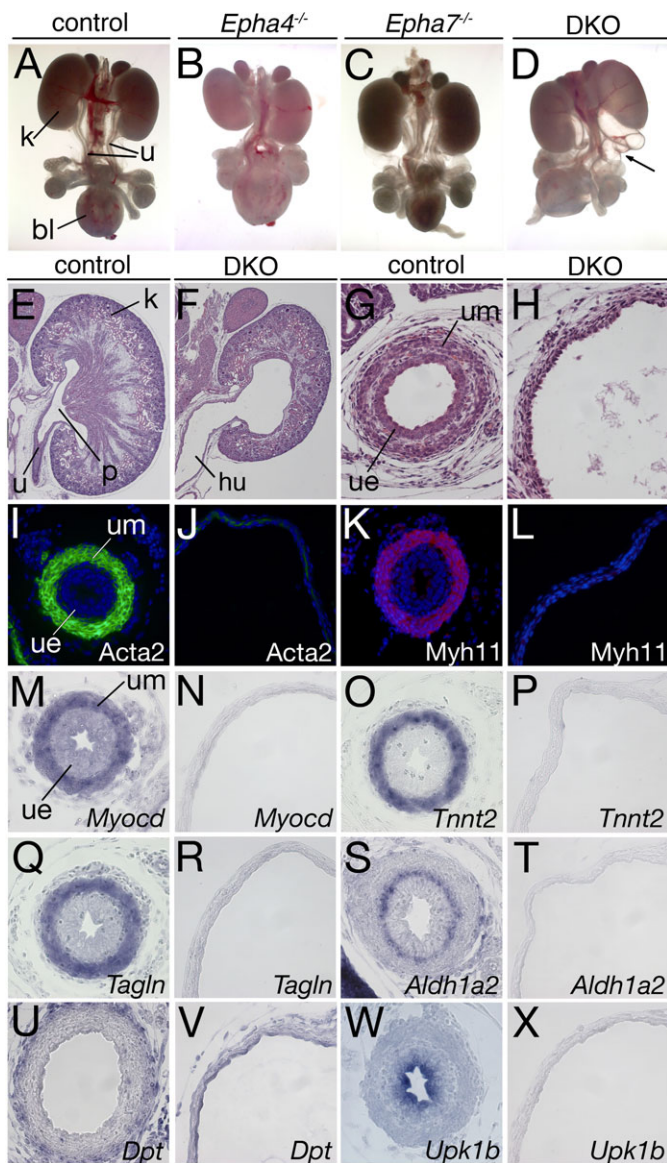
Fig. 2. Kidney and ureter anomalies in *Epha4*$^{-/-}$;*Epha7*$^{-/-}$ (DKO) embryos at E18.5. (A-D) Morphology of whole urogenital systems of male embryos. (E-H) Hematoxylin and Eosin stainings of sagittal sections of kidneys (E,F) and of transverse sections of the proximal ureter (G,H). (I-X) Cytodifferentiation of the ureteric mesenchyme (I-V) and epithelium (W,X) as shown by immunofluorescence (I-L) and *in situ* hybridization analysis (M-X) on transverse sections of the proximal ureter at E18.5. bl, bladder; hu, hydroureter; k, kidney; p, pelvis; u, ureter; ue, ureteric epithelium; um, ureteric mesenchyme.

hydroureter and/or megaureter with hydronephrosis (Fig. 2D; supplementary material Fig. S2A,B). Quantification of the gross morphological defects of the urogenital system of embryos of both genotypes uncovered sex independence but an incomplete penetrance (47% in DKO and 19% in *Epha4*$^{-/-}$;*Epha7*$^{+/-}$ mice) and variability (unilateral and/or bilateral hydroureter and/or megaureter) (supplementary material Table S1).

Histological analyses of DKO and *Epha4*$^{-/-}$;*Epha7*$^{+/-}$ urogenital systems with megaureter revealed dilatation of the entire renal collecting system including the collecting ducts, calyx, pelvis and the absence of the papilla. The ureter was strongly dilated and featured a flat and single-layered urothelium with a thin layer of surrounding mesenchyme (Fig. 2E-H; supplementary material Fig. S2C-H).

To characterize the cellular changes associated with megaureter formation in DKO mice, we analyzed the expression of cell differentiation markers within the epithelial and mesenchymal compartments at the proximal ureter level at E18.5. In the mesenchymal compartment, expression of SM structural proteins (Acta2 and Myh11), of genes encoding SM structural components (*Tagln* and *Tnnt2*), and of the key regulator of SM cell differentiation, *Myocd*, was absent. *Aldh1a2*, a marker for the lamina propria, was not expressed. *Dpt*, a marker for the outer adventitial layer of fibroblasts, was severely reduced (Fig. 2M-V). Epithelial differentiation was also affected in the mutant, as shown by the strong reduction of the urothelial marker *Upk1b* (Fig. 2W,X).

Expression of all of these markers was similarly absent at proximal levels of *Epha4*$^{-/-}$;*Epha7*$^{+/-}$ megaureters (supplementary material Fig. S2I-T), indicating that megaureter formation is associated with a failure of cytodifferentiation along the entire tube in both genotypes. By contrast, the hydroureter phenotype in DKO embryos was associated with a slight reduction of SM markers and unchanged expression of *Upk1b* at proximal levels (supplementary material Fig. S3). We conclude that combined loss of *Epha4* and *Epha7* results in severe defects of ureteric cytodifferentiation that correlate with the degree of dilatation.

Onset and progression of ureter defects in DKO embryos

To further explore the relationship between cytodifferentiation defects of DKO ureters and urinary pressure, we analyzed urogenital systems at E14.5, E15.5 and E16.5, i.e. before, at and after the onset of urine production in the kidneys. On the morphological and histological level, the urogenital systems of DKO embryos showed no defects at E14.5 and E15.5, whereas ureter and pelvicalyceal dilatation was detectable at E16.5 (supplementary material Fig. S4A-C). Expression of *Myocd* was initiated at E14.5 and maintained at E15.5 and expression of *Tagln*, *Tnnt2*, *Myocd* and *Upk3b* was observed at E15.5 in DKO ureters, indistinguishable from the control. However, SM and urothelial markers were collectively downregulated in DKO ureters at E16.5 (supplementary material Fig. S4D,E). Furthermore, the expression of genes required in the undifferentiated ureteric mesenchyme to initiate the SM differentiation program was unaffected in DKO ureters at E14.5 (supplementary material Fig. S5). This suggests that *Epha4* and *Epha7* are not required (downstream of *Tbx18*) in the undifferentiated ureteric mesenchyme to initiate the SM differentiation program. Loss of cytodifferentiation in DKO embryos is most likely a consequence and not a cause of increased hydrostatic pressure and might relate to physical obstruction along the ureter.

Aberrant ureter-bladder connectivity in DKO embryos

To test for the continuity of the ureter and the patency of its junctions, we injected ink into the renal pelvis in isolated urogenital systems of E18.5 embryos. In control embryos, the ink passed readily through the ureter and filled the entire bladder (*n*=4; Fig. 3A). In the megaureter situation of DKO embryos, the ink was either retained within the ureter that ended blindly or on the vas deferens (*n*=3; Fig. 3B), or the ink accumulated within a sac in the bladder to be released through the urethra (*n*=2; Fig. 3C). In the DKO situation with hydroureter, the ink was retained in the ureter that terminated on the urethra (*n*=1; data not shown). Serial histological sections and 3D reconstructions revealed that in control embryos the distal ureters entered the bladder at an oblique angle at the dorsal bladder neck and the lumen was continuous (*n*=3; Fig. 3D,G). In DKO embryos with megaureter, the distal ureters ended as an intravesical (*n*=3) or an extravesical (*n*=2) pouch-like
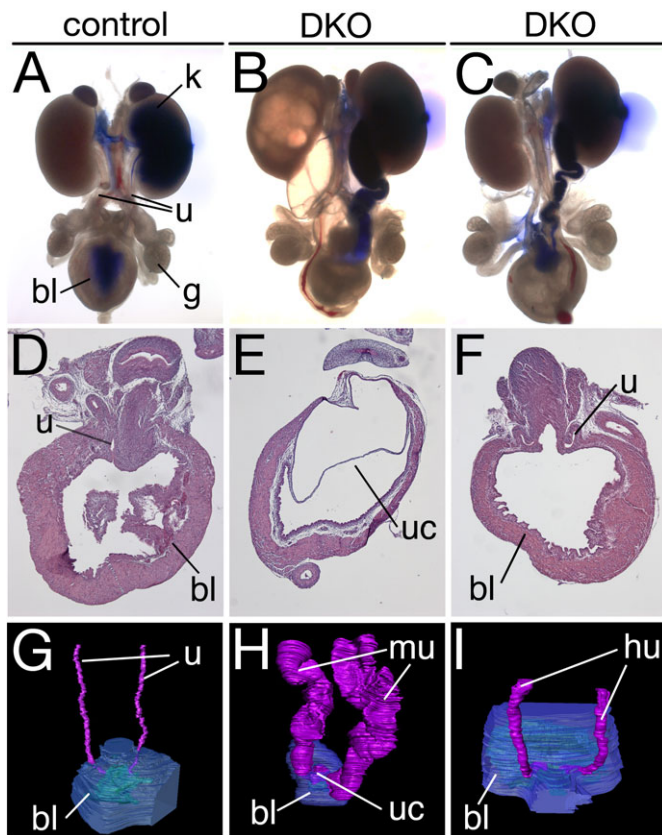
Fig. 3. Vesico-ureteric junction (VUJ) anomalies in DKO embryos at E18.5. (A-C) Distribution of ink injected in the pelvic region of whole urogenital systems. (D-F) Hematoxylin and Eosin stainings of frontal sections of the bladder. (G-I) Three-dimensional reconstructions of serial histological sections of the ureter (pink), the bladder muscle (blue) and the bladder lumen (green). bl, bladder; hu, hydroureter; k, kidney; mu, megaureter; g, gonad (testis); u, ureter; uc, ureterocele.

structure, termed the ureterocele (Fig. 3E,H; data not shown). In the case of hydroureter, the distal ureter terminated ectopically in the urethra (n=2; Fig. 3F,I). We conclude that anatomical obstruction caused by aberrant connectivity of the bladder and the distal ureter underlies hydro/megaureter in DKO embryos.

Defects in fusion of the ND with the cloaca

In order to elucidate the morphogenetic origin of this aberrant ureter-bladder connectivity, we analyzed urogenital systems by 3D reconstruction of serial histological sections at earlier embryonic stages (Fig. 4). At E10.5 in the wild type, the UB had emerged from the ND and the CND was fused with the cloaca. In DKO embryos, the position of the UB was unaffected; the CND approached the cloaca in the midline but contact and fusion of the two epithelia either occurred ectopically in a more anterior position (n=3) or was not detected at all (n=2) (Fig. 4A,B). In E12.5 wild-type embryos, the CND was still present and fused with the urogenital sinus but the lumen was not yet continuous. In all DKO embryos analyzed the CND was present but appeared longer than in controls (supplementary material Fig. S6). In three of five, cases the CND was fused with the primitive bladder, whereas a gap between the CND and the urogenital sinus was observed in two specimens (Fig. 4C,D). In E13.5 and E14.5 wild-type embryos, the CND was eliminated and the distal ureter and the ND were well separated; they were inserted into the bladder but the lumen was not yet continuous. In the DKO situation, the CND persisted and gained an ampulla-like

swelling within the bladder wall at these stages (Fig. 4E-I), as confirmed by GFP epifluorescence using the *Hoxb7-GFP* reporter line, which marks the ND and all of its descendants (Fig. 4J) (Srinivas et al., 1999). In four of five cases the CND was fused with the urogenital sinus, whereas in one specimen a gap between the two epithelia was still detectable. We suggest that ureterocele and megaureter in DKO embryos is caused by the persistence of the CND, which in turn results from a failure or delayed fusion of the ND with the cloaca.

Cellular changes in the distal ND of DKO embryos

To analyze the cellular changes in the mutant ND in more detail, we performed live cell imaging of explants of E9.5 trunks of embryos carrying the *Hoxb7-GFP* transgene. At E9.5, the tip of the ND was characterized by the presence of cellular protrusions both in wild-type and in DKO embryos, as previously reported (Chia et al., 2011). During the 18 h culture period these protrusions were highly dynamic, switching between extension and retraction cycles, but remained associated with a compact tip that moved progressively forward in the wild type. By contrast, in DKO embryos, individual cells dramatically stretched during the formation of these protrusions and started to lose contact with the tip of the ND after 5 h of culture to finally scale off [n=3; Fig. 5A-D; supplementary material Movies 1A,B (control) and 2A,B (DKO)].

Confocal immunofluorescence analysis on sections of E10.5 embryos confirmed these observations. In wild-type embryos, GFP expression from the *Hoxb7-GFP* transgene was confined to cells of the distal ND, whereas in DKO embryos GFP-positive cell material was additionally found in the periphery of the distal ND (Fig. 5E,F). Furthermore, collagen type IV (ColIV) staining revealed an uninterrupted basal lamina underlying the ND in the wild type, whereas several gaps were detected in DKO embryos (Fig. 5G,H). Finally, Cdh1, a marker for basolateral membranes of epithelial cells, was severely downregulated in DKO embryos (Fig. 5I,J), supporting the notion that tissue integrity is perturbed in the distal ND of DKO embryos.

Analysis of the expression of endothelial [endoglin (*Eng*), vimentin (*Vim*), endomucin (Emcn)] and neuronal [*Hand2*, neuropilin 1 (Nrp1), neurofilament light chain (Nefl)] markers (supplementary material Fig. S7) did not detect differences in the mesenchymal tissue surrounding the E10.5 ND between wild-type and DKO embryos, arguing against the possibility that changes in endothelial and neuronal networks have misguided the ND in DKO embryos.

Previous studies have shown that distal ureter maturation requires the apoptotic removal of the CND (Batourina et al., 2002, 2005; Uetani et al., 2009). Analysis of programmed cell death by the TUNEL assay revealed that in wild-type embryos apoptosis was initiated at E10.5 and maintained at E12.5 in the CND. Apoptosis was similarly observed in the CND of DKO embryos, in which the CND was fused with the cloaca/bladder epithelium. By contrast, apoptosis was absent in specimens in which the CND was separated from the cloaca (supplementary material Fig. S8). Together, these findings suggest that EphA4/EphA7 signaling is required to maintain adhesion between ND tip cells to allow fusion with the cloaca, which in turn is prerequisite for the stepwise apoptotic removal of the CND until E13.5.

Perturbation of the *Ret/Gata3* molecular network in the caudal ND in DKO embryos

To determine molecular changes that are associated with the fusion defect of the caudal ND in DKO embryos, we analyzed
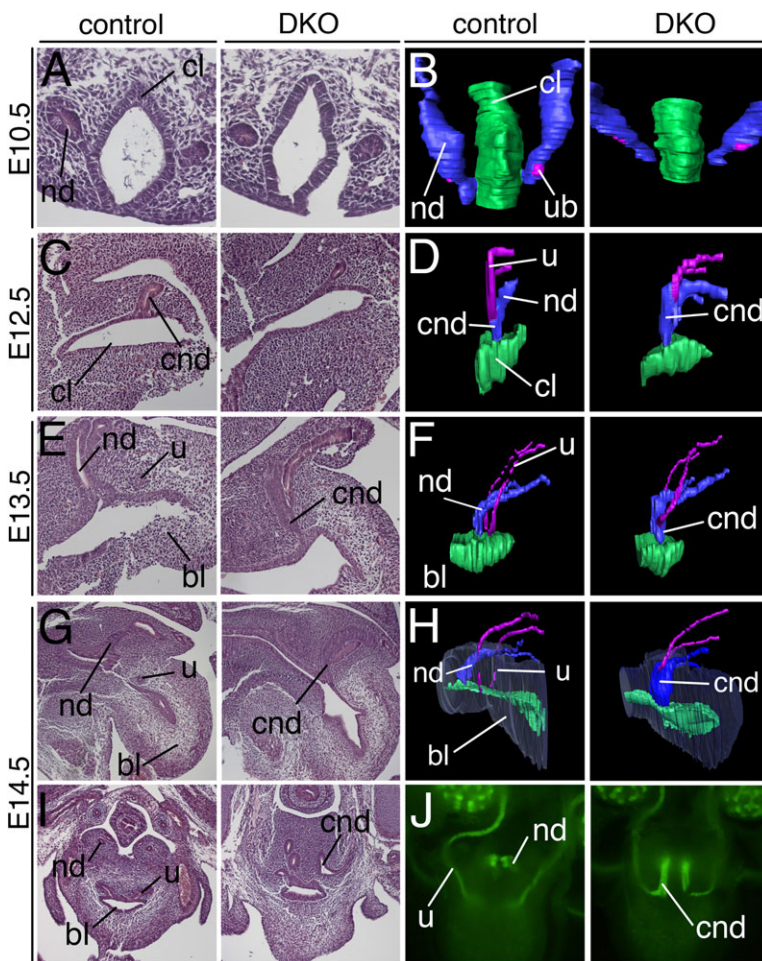
**Fig. 4. Onset of VUJ anomalies in DKO embryos.**
(A,C,E,G,I) Histological analysis by Hematoxylin and Eosin staining of transverse (A,I) and sagittal (C,E,G) sections at the junction between the developing bladder and the distal ND and ureter. (B,D,F,H) Three-dimensional reconstructions of serial histological sections of the distal ND (blue), ureter (pink) and bladder region (bladder lumen in green, bladder wall in transparent gray). (J) GFP epifluorescence of ND derivatives marked by the *Hoxb7-GFP* reporter. (A,B) Dorsal is up; (C-H) anterior is to the left, dorsal is up. bl, bladder; cl, cloaca; cnd, common nephric duct; nd, nephric duct; u, ureter; ub, ureteric bud.

the expression of a panel of genes previously implicated in ND extension and fusion in E9.5 whole embryos and on sections through the posterior trunk of E10.5 embryos. At E9.5 (when the ND has reached the cloacal level) expression of *Pax2*, *Gata3* (not shown), *Lhx1* and *Ret* was found along the entire ND of DKO embryos, indistinguishable from controls (Fig. 6A-D). At E10.5 the expression of *Emx2* was unaffected, whereas *Pax2* was slightly diminished, and *Lhx1*, *Gata3* and *Ret* were severely reduced in the caudal ND of DKO embryos (Fig. 6E-P). Expression of *Gdnf*, which encodes the ligand of the Ret receptor (Treanor et al., 1996), was restricted to the metanephric blastema both in wild-type and DKO embryos (Fig. 6K,L). As expression of *Ret* also depends on RA signaling (Chia et al., 2011), we analyzed expression of the genes encoding the biosynthetic enzyme Aldh1a2 and the receptor and target of RA signaling Rarb (Matt et al., 2003). Expression of *Aldh1a2* in the pericloacal mesenchyme of DKO embryos was unaltered, whereas expression of *Rarb*, which in control embryos is restricted to the fusion site in the cloacal epithelium, appeared scattered and reduced (Fig. 6Q-T). Expression of *Ptch1*, which is a target of Hedgehog signaling (Ingham and McMahon, 2001), in the pericloacal mesenchyme, and of *Shh* in the cloacal epithelium was observed in both wild-type and DKO embryos (Fig. 6U-X). Expression of ND marker genes was not affected on more anterior metanephric and mesonephric levels in DKO embryos (supplementary material Fig. S9), indicating that pericloacal EphA4/EphA7 signaling affects the *Lhx1/Gata3/Ret* network specifically in the adjacent caudalmost aspect of the ND.

The caudal ND is the target of pericloacal mesenchymal EphA4/EphA7 signaling

Failure of ND insertion might indicate a non-cell-autonomous requirement of pericloacal mesenchymal EphA4/EphA7 signaling in the epithelium of the cloaca and/or the caudal ND to regulate adhesion and/or fusion within and between the two compartments. In order to determine the target tissue of EphA4/EphA7 signaling in the lower urinary tract, we incubated E9.5 wild-type embryos with fusion proteins of the soluble part of EphA4 or EphA7 with the constant domain of antibodies and subsequently recorded the distribution of the bound ligand by anti-IgG-AP fusion protein-mediated enzymatic detection (Gale et al., 1996). EphA4 and EphA7 binding patterns were virtually identical and comprised the branchial arches, the ventral forebrain, the forelimb bud and – most relevant to this project – the caudal ND and the cloaca (Fig. 7A,B). To identify ligand(s) of EphA4 and/or EphA7, we screened for expression of all known ephrin A and ephrin B genes by section RNA *in situ* hybridization analysis at E10.5 (supplementary material Fig. S10). Expression of ephrin B2 (*Efnb2*), which encodes a known ligand of EphA4 signaling (Watanabe et al., 2009), was found in the caudal ND and the cloaca as well as in the pericloacal mesenchyme from E10.5 until E14.5 (Fig. 7C-F). Immunofluorescence analysis confirmed these expression domains and identified membranous localization of ephrin B2 protein in the epithelia of the ND and the cloaca and in endothelial cells (Fig. 7G).

In order to determine whether the signal that results from binding of EphA4/EphA7 to ephrin B2 was transduced into the ligand-bearing cell, we performed anti-phospho-ephrin B (Y316) antibody
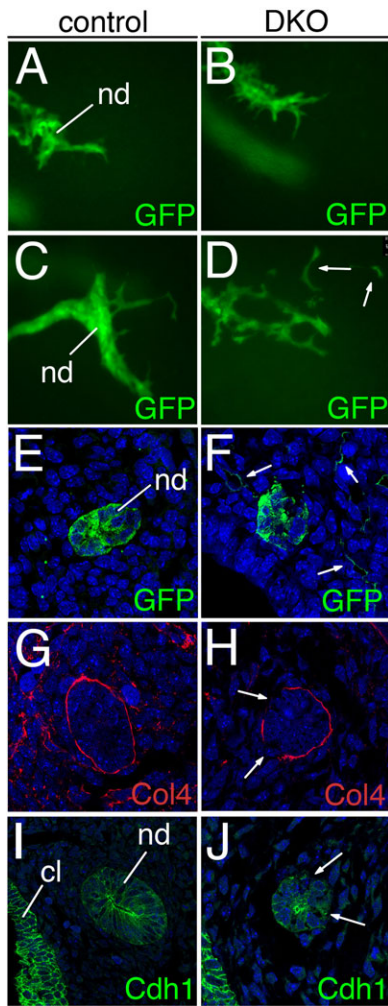
Fig. 5. Cellular changes in the caudal ND of DKO embryos at E9.5 and E10.5. (A-D) GFP epifluorescence of the caudal ND visualized by the *Hoxb7-GFP* reporter in explants of E9.5 trunk at the onset of the culture (A,B) and after 18 h (C,D). (E-J) Confocal analysis on transverse sections through the distal ND region by immunofluorescence for GFP (E,F), the basal lamina marker Col4a4 (G,H), and the epithelial marker Cdh1 (I,J). Arrows point to scaled off ND cells (D,F), to disruption of the basal lamina (H), and to disrupted epithelial integrity (J). nd, nephric duct; cl, cloaca.

staining. This specific tyrosine phosphorylation site has been described to activate downstream Src family or associated kinases as a result of active ephrin B reverse signaling (Palmer et al., 2002; Wu et al., 2011; Georgakopoulos et al., 2011). In the wild type, we found phospho-specific staining in membranes of epithelial cells of the ND, the cloaca and endothelial cells at E10.5, whereas strongly reduced phospho-specific staining was detectable in the ND and the cloaca in the DKO situation (Fig. 7H,I). Taken together, these findings argue for active EphA4/EphA7-ephrin B2 reverse signaling in the ND and cloacal epithelium.

Loss of *Efnb2* in the ND leads to urinary tract anomalies

To determine whether ephrin B2 is functionally involved in ND development, we used a conditional gene targeting approach with a floxed allele of *Efnb2* (*Efnb2^fl^*) and a *Pax2(8.5)-cre* driver line that mediates specific recombination in the ND and its derivatives (supplementary material Fig. S11) (Kuschert et al., 2001; Trowe et al., 2011). At E18.5, *Pax2(8.5)-cre;Efnb2^fl/fl^* embryos (*n*=17) displayed urinary anomalies in 60% of specimens analyzed. These
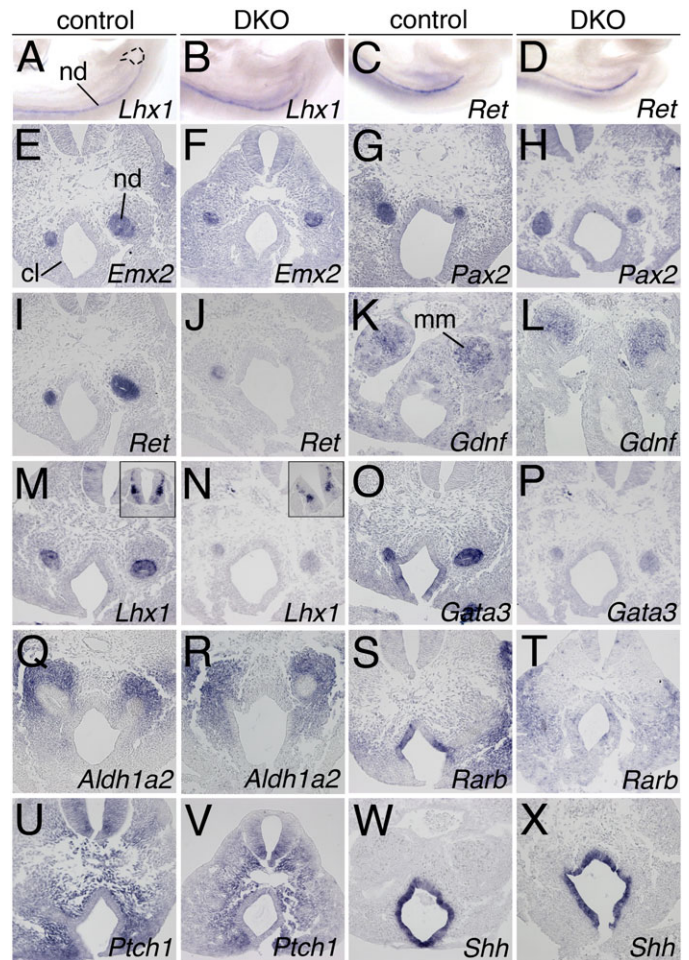

Fig. 6. Molecular changes in the ND of DKO embryos at E9.5 and E10.5. RNA *in situ* hybridization analysis on whole E9.5 embryos (A-D) and on transverse sections of the posterior trunk of E10.5 embryos (E-X). Dashed line in A outlines the cloaca. Insets (M,N) show the neural tube. nd, nephric duct; cl, cloaca; mm, metanephric mesenchyme.

anomalies were sex independent and included bilateral hydroureter (*n*=7) and unilateral megaureter (*n*=3) (Fig. 8A-D; supplementary material Table S2). Histological analysis of mutant urogenital systems revealed a strong dilatation of the ureter and renal pelvis with occasional absence of the renal papilla (Fig. 8E,F). In order to unravel a potential physical obstruction in *Efnb2*-deficient embryos, we performed histological analysis of sagittal bladder sections at E18.5 to visualize the VUJ. In mutant specimens with CAKUT-like phenotypes (*n*=7), we found distal ureters that were embedded in the bladder muscle but were without connection to the bladder lumen (*n*=3) or distal ureters that terminated in the urethra (*n*=1) (Fig. 8G,H; data not shown). This suggests physical obstruction as the cause of hydroureteronephrosis.

To determine the status of CND removal, we investigated sagittal sections of the E14.5 urogenital sinus. In wild-type embryos (*n*=4) the CND was eliminated and ND and ureter were separated. In mutant embryos (*n*=4), the CND was either still present and fused with the urogenital sinus (*n*=1) or the CND was eliminated but the ND and ureter were not well separated (*n*=1) (Fig. 8I,J; data not shown). Moreover, we found ND fusion defects (mainly unilaterally) at E10.5 in three out of five *Pax2(8.5)-cre;Efnb2^fl/fl^* mutants analyzed, similar to DKO embryos (Fig. 8K,L). Molecular markers associated with ureter SM development were unchanged in
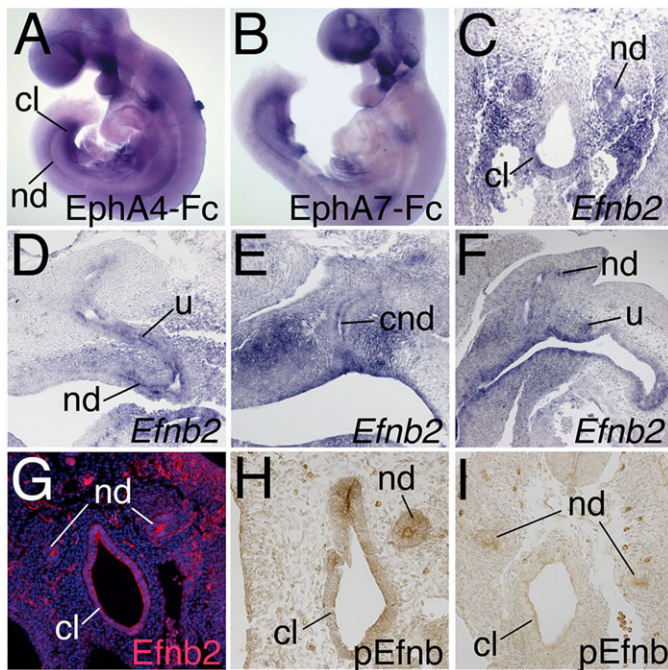
Fig. 7. The ND is a target of pericloacal EphA4/EphA7 reverse signaling. (A,B) Whole-mount EphA4/EphA7-Fc staining of E9.5 wild-type embryos. (C-F) *Efnb2* expression analysis by RNA *in situ* hybridization on a transverse section of a E10.5 posterior trunk (C), and on sagittal sections through the posterior trunk region at E11.5 (D), E12.5 (E) and E14.5 (F). (G) Efnb2 immunofluorescence on sections of wild-type embryos at E10.5. (H,I) Immunohistochemistry of phosphorylated ephrin B (pEfnb) on transverse sections of wild-type (H) and DKO (I) embryos at E10.5. nd, nephric duct; cl, cloaca; u, ureter.

Fig. 8. Loss of *Efnb2* in the ND leads to CAKUT-like phenotypic changes. (A-D) Morphology of urogenital systems of male (A,B) and female (C,D) E18.5 embryos. (E-L) Hematoxylin and Eosin stainings of sagittal sections of E18.5 kidney (E,F) and bladder (G,H), of the E14.5 urogenital sinus (I,J), and of transverse sections of E10.5 trunk (K,L). Arrows (B,D,H) indicate hydroureter in the mutant. k, kidney; u, ureter; bl, bladder; p, pelvis; cl, cloaca; nd, nephric duct; cnd, common nephric duct.

Pax2(8.5)-cre;Efnb2^{fl/fl} embryos at E14.5 (supplementary material Fig. S12). We conclude that Efnb2, similar to EphA4/EphA7, is required to establish proper ureter-bladder connectivity by promoting ND insertion into the cloaca.
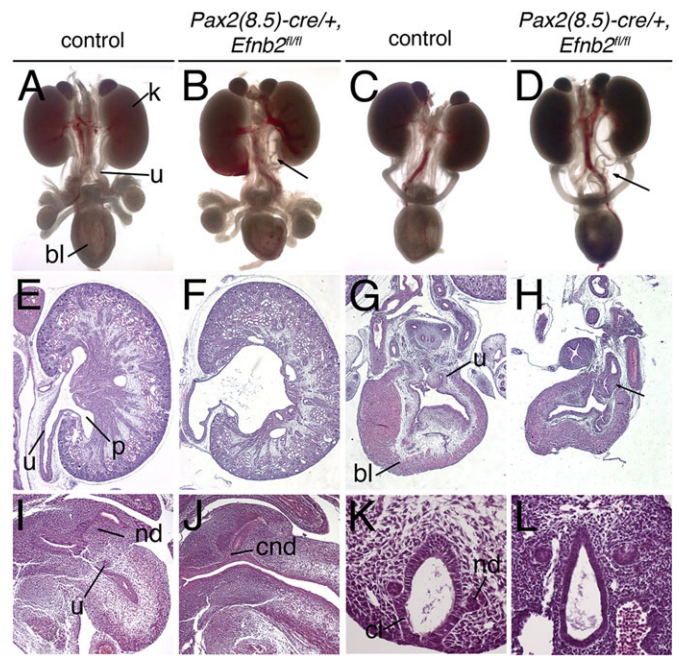
Loss of *Lhx1* and downregulation of *Gata3* expression in the distal ND of *Pax2(8.5)-cre;Efnb2^{fl/fl}* embryos

We next sought to elucidate whether the loss of *Efnb2* in the ND results in similar molecular changes as observed in DKO embryos. We performed RNA *in situ* hybridizations on sections of E10.5 posterior trunks with the previously employed panel of genes associated with ND extension or fusion. Marker expression was unchanged at the mesonephros level (supplementary material Fig. S13). At the cloacal level, *Emx2*, *Pax2* and *Axin2* expression was unaltered, but expression of *Gata3* and *Lhx1* was strongly diminished and that of *Ret* was slightly reduced in the caudal ND of *Pax2(8.5)-cre;Efnb2^{fl/fl}* embryos (Fig. 9K,L). Expression of *Aldh1a2* and *Ptch1* in the pericloacal mesenchyme and of *Rarb* and *Shh* in the cloacal epithelium was unaffected at this stage in the mutant. Taken together, these findings confirm *Lhx1*, *Gata3* and *Ret* as molecular targets of ephrin B2 signaling in the caudal ND.

DISCUSSION
Pericloacal Eph signaling maintains caudal ND integrity via the *Lhx1/Gata3/Ret* network

ND elongation and fusion are poorly defined processes that depend on permissive and instructive cues from surrounding tissues (Drawbridge et al., 2000; Morris et al., 2003; Obara-Ishihara

et al., 1999). These cues are likely to be sensed by a specialized tip that translates them into directional growth towards and integration into the cloaca. Recent live cell imaging revealed the presence of protrusions at ND tip cells, similar to growth cones of nerve cells (Chia et al., 2011). Our videomicroscopy confirmed these tip cell protrusions and revealed that they switch dynamically between extension and retraction during ND migration. In DKO embryos, the ND tip was similarly dynamic in the formation of cellular protrusions during most of the posterior extension, but cells detached from the tip cell community in the last phase of migration once they had turned towards the cloaca in the midline of the embryo. Unfortunately, we were not able to simultaneously visualize the cloacal epithelium in our explant system in order to relate the cellular changes of the ND tip with the presence of the cloaca. Therefore, we cannot exclude the possibility that the disintegration of the ND tip is the consequence rather than the cause of failed interaction with the cloaca. However, we consider it more likely that ND tip disintegration precedes contact with the cloaca, as our molecular analysis showed that factors known to be required for caudal ND extension are collectively downregulated and that the cloacal epithelium seems largely unaffected.

Our molecular analysis identified *Ret*, *Gata3* and *Lhx1* as targets of EphA4/EphA7 signaling in the ND tip. Loss of *Gata3*, *Ret* and *Aldh1a2* has recently been associated with the absence of cellular protrusions of ND tip cells and a failure of ND integration. It was suggested that *Gata3* in the ND and RA signaling from the pericloacal mesenchyme act in parallel to maintain *Ret* expression in the caudal ND (Chia et al., 2011). *Lhx1* has also been shown to be required for the caudal portion of the ND to reach the urogenital sinus. It appears to act upstream of *Ret* but independently of *Gata3* (Pedersen et al., 2005), arguing
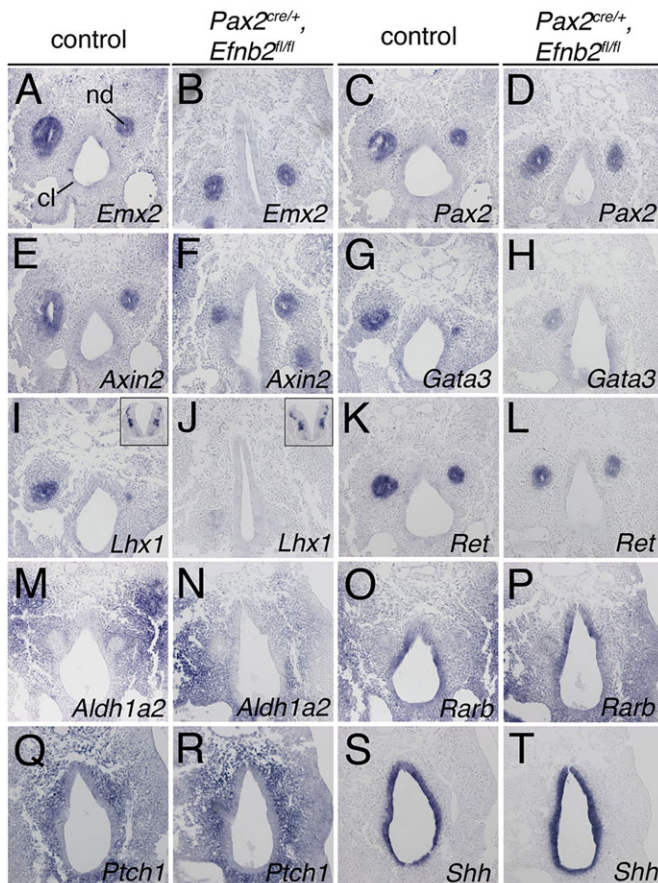
Fig. 9. Molecular changes in the caudal ND of *Pax2(8.5)-cre/+;Efnb2^{fl/fl}* embryos at E10.5. RNA *in situ* hybridization analysis of genes associated with ND extension or fusion on transverse sections of posterior trunks of E10.5 embryos. Insets (I,J) show spinal cord expression as an internal control. nd, nephric duct; cl, cloaca.

together that *Gata3* and *Lhx1* represent the primary targets of Eph/ephrin activity in the ND.

EphA4/EphA7 act in *trans* via ephrin B2-mediated reverse signaling

Eph/ephrin signaling represents an unusual intercellular communication module in the sense that the signals can elicit molecular changes both in the receptor-bearing as well as the ligand-bearing cell. As our study suggests that the caudal ND is the crucial target of EphA4/EphA7 activity in the pericloacal mesenchyme, it is possible that EphA4/EphA7 control the expression of a diffusible ligand in the pericloacal mesenchyme by forward signaling. Alternatively, EphA4/EphA7 might use the reverse signaling mode to directly activate transcriptional and/or cytoskeletal changes in the caudal ND. For a number of reasons, we deem the second possibility more likely. First, we found binding of EphA4/EphA7 to cells in the ND and the cloaca but not in the pericloacal mesenchyme. Second, specific expression of the ephrin B2 ligand was found in these two tissue compartments. Third, ephrin B2 signaling was greatly reduced in these compartments in mice with combined loss of *Epha4* and *Epha7*. Fourth, the observed loss of cell adhesion between ND tip cells is more compatible with the known role of reverse signaling in mediating adhesive cell interactions than with cell repulsion, which has been recognized as a consequence of Eph forward signaling (Kao et al., 2012).

Intriguingly, reverse ephrin B2 signaling has been implicated in the control of epithelial cell adhesion in urorectal maturation by promoting tubularization of the urethra and septation of the urinary and the anorectal system (Dravis et al., 2004). Fifth, although EphA receptors preferentially bind to ephrin A ligands, ephrin B2 has been described as a ligand for EphA4 in some contexts (Watanabe et al., 2009); ephrin B2 binding to EphA7 still needs to be validated on the biochemical level. Last, and most importantly, conditional deletion of *Efnb2* in the ND phenocopied the urinary tract defects of DKO embryos to a substantial extent, including blind or ectopically ending ureters, delayed CND removal, lack or delayed ND insertion and downregulation of *Gata3/Lhx1/Ret* in the caudal ND.

It remains to be seen how ephrin B2 signaling maintains the expression of *Gata3* and *Lhx1* and adhesion between cells in the ND tip. MAPKs, such as Erk1/2 (Mapk3/1), act downstream of ephrin B2-activated Src kinases but are also the main downstream signaling pathway activated by receptor tyrosine kinases including Ret (Hoshi et al., 2012; Sebolt-Leopold and Herrera, 2004). Independent of the precise epistatic relationship or of direct phosphorylation by Src kinases or by Ret, MAPK signaling might control the cytoskeletal changes that confer adhesive properties between ND tip cells.

EphA4/EphA7 signaling is also transduced into the cloacal epithelium, suggesting that ephrin B2 mediates some kind of heterotypic adhesion between the ND and the cloaca. Thus far, we have not found direct evidence for this hypothesis, as expression of cell adhesion molecules in the two compartments was unaffected and the integrity of the cloacal epithelium was preserved in DKO embryos.

We also observed reduced *Rarb* expression, a target gene of RA signaling in the cloacal epithelium (Tsou et al., 1994). RA is produced in the pericloacal mesenchyme by Aldh1a2. We did not find a change in the expression of *Aldh1a2* in the pericloacal mesenchyme of DKO embryos, but this might be due to the insensitivity of the *in situ* hybridization technique to detect small expression changes. Hence, it is conceivable that RA is reduced as a consequence of disturbed EphA4/EphA7 forward signaling in the pericloacal mesenchyme, resulting in reduced activation of RA target genes such as *Rarb* and also *Ret* in the caudal ND and cloaca.

A previous study revealed that, during the establishment of limb innervation by motor neurons, Ret and EphA signaling do not act in series but in parallel (Kramer et al., 2006). Gdnf from the dorsal limb bud mesenchyme acts as an attractive cue for motor neurons via binding to the Ret receptor. Ret additionally seems to act as a co-receptor for attractive reverse ephrin A signaling, thus integrating two attractive cues for pathfinding (Bonanomi et al., 2012). A similar interaction might hypothetically guide the ND to its target tissue. However, we did not detect *Gdnf* expression in the cloaca or pericloacal mesenchyme but in the metanephric blastema. In summary, we suggest that reverse ephrin B2-mediated EphA4/EphA7 signaling from the pericloacal mesenchyme maintains via the *Lhx1/Gata3/Ret* network the epithelial integrity of the ND tip, which is required for proper fusion with the cloaca.

ND defects underlie aberrant VUJ and ureter dilatation

DKO and *Pax2(8.5)-cre/+;Efnb2^{fl/fl}* embryos exhibited with ~50% penetrance a continuum of upper urinary tract defects ranging from weak unilateral hydroureter to strong bilateral megaureter. Our molecular analysis excluded a functional obstruction as the causative agent. However, we detected a range of VUJ malformations that corresponded in severity to the dilative uropathies: megaureters were associated with ureterocele and blind-ending ureters, and hydroureters

with ureters ending ectopically (e.g. in the urethra). Such a range of structural malformation and penetrance seems unusual for a monogenetic disease and might indicate genetic interaction with as yet unknown factors, or might stem from the mosaic composition of the genetic background that we obtained by continuous outcrossing from an initially C57BL/6 background. However, as we obtained the same range of structural malformation after each outcrossing, we consider it more likely that it simply relates to slight variations in the extension of the ND resulting in the absent, delayed or ectopic fusion with the cloaca that occurred in 100% of DKO embryos analyzed at E10.5. Lack of ND integration impaired CND removal by apoptosis and ureters remained attached to the NDs. Following massive growth of the bladder, the CND became incorporated into the bladder resulting in intravesical ureterocele, or remained outside ending blindly, resulting in hydroureter/megaureter and associated hydronephrosis upon onset of urine production in the kidney. By contrast, delayed or ectopic fusion of the ND with the cloaca may result in ureters ending ectopically with much less severe phenotypic manifestations at E18.5, or might be partially or completely resolved during further morphogenetic steps. These findings strongly support the conclusions of a recent study of mice mutant for *Ret*, *Gata3* or *Aldh1a2*, which reported that a defect in ND integration is a novel cause of CAKUT (Chia et al., 2011).

It was recently reported that mice deficient for a mutant allele of *Epha4* exhibit spontaneous hydronephrotic lesions in adulthood. The low rate (17%) and late onset (3-10 months) of the defects strongly support our findings that *Epha4* and *Epha7* act redundantly to establish a proper VUJ (Sallstrom et al., 2013).

MATERIALS AND METHODS

Microarray analysis
Preliminary microarray analysis used for the identification of candidate genes was performed by the core facility Transcriptomics of Medizinische Hochschule Hannover using Agilent mouse whole-genome arrays with RNA isolated from E13.5 wild-type and *Tbx18*-deficient ureters.

Mice
Mice carrying null alleles for *Tbx18* (*Tbx18*^tm2Akis^; synonym *Tbx18*^GFP^) (Christoffels et al., 2006), *Epha4* (*Epha4*^tm1Pvan^; synonym *Epha4*^−^) (Kullander et al., 2001) and *Epha7* (*Epha7*^tm1Ud^; synonym *Epha7*^−^) (Dufour et al., 2003), mice with a floxed allele of *Efnb2* (*Efnb2*^tm4Kln^; synonym *Efnb2*^fl^) (Grunwald et al., 2004), transgenic mouse lines *Hoxb7-GFP* [*Tg(Hoxb7-EGFP)33Cos*] (Srinivas et al., 1999) and *Pax2(8.5)-cre* (Trowe et al., 2011), and the double fluorescent Cre reporter line *Gt(ROSA) 26Sor*^tm4(ACTB-tdTomato,-EGFP)Luo^ (synonym *R26*^mTmG^) (Muzumdar et al., 2007) were maintained on an NMRI outbred background. *Epha4/Epha7* compound mutant mice were obtained from matings of *Epha7*^−/−^;*Epha4*^+/−^ males and *Epha4*^+/−^;*Epha7*^+/−^ or *Epha7*^−/−^;*Epha4*^+/−^ females. *Epha7*^+/−^; *Epha4*^+/+^ and *Epha7*^+/−^;*Epha4*^+/−^ littermates were interchangeably used as controls. *Pax2(8.5)-cre/+;Efnb2*^fl/fl^ embryos were obtained from matings of *Pax2(8.5)-cre/+;Efnb2*^fl/+^ males with *Efnb2*^fl/+^ females. Embryos for Eph/ephrin gene expression analysis were derived from matings of NMRI wild-type and *Tbx18*^GFP/+^ mice. For timed pregnancies, vaginal plugs were checked in the morning after mating; noon was taken as E0.5. Pregnant females were sacrificed by cervical dislocation; embryos were harvested in phosphate-buffered saline (PBS), decapitated, fixed in 4% paraformaldehyde/PBS overnight, and stored in 100% methanol at −20°C before further use. Genomic DNA prepared from tails or embryonic tissues was used for genotyping by PCR.

Morphological, histological and immunohistochemical analyses
Ink injection experiments were performed as previously described (Airik et al., 2010). For histological stainings, organ rudiments or posterior trunks of embryos were paraffin embedded and sectioned at 5 μm. Sections were stained with Hematoxylin and Eosin. Three-dimensional (3D) reconstruction of stained serial sections was performed according to published protocols (Soufan et al., 2003).

For Eph receptor-Fc stainings, we modified a previously published protocol (Gale et al., 1996). E9.5 embryos were incubated with recombinant mouse EphA4-Fc or recombinant mouse EphA7-Fc chimeric proteins (#641-A4-200 and #608-A7-200, R&D Systems). For detection of Eph-Fc binding, embryos were incubated with anti-human IgG (H&L) AP conjugate (#S3821, Promega; 1:1500). Embryos were stained with either NBT/BCIP or INT/BCIP (#11681451001 or #11681460001, Roche Diagnostics) in the dark. To permeabilize the tissue, we used Tween 20 in the wash buffer.

For the detection of antigens on 5 μm paraffin sections, the following primary antibodies and dilutions were used: anti-Myh11 (kindly provided by R. Adelstein, NIH, Bethesda, MD, USA; 1:400), mouse anti-Acta2 (#F3777 and C6198, Sigma; 1:200), rabbit anti-Cdh1 (kindly provided by R. Kemler, MPI for Immunobiology and Epigenetics, Freiburg, Germany; 1:200), rabbit anti-ephrin B2 (#sc-15397, Santa Cruz; 1:200), rabbit anti-phospho-ephrin B (Y316) (#PPS047, R&D Systems; 1:50), rat monoclonal anti-endomucin (kindly provided by D. Vestweber, MPI for Molecular Biomedicine, Münster, Germany; 1:10), mouse monoclonal anti-neurofilament (DSHB; 1:200), rat anti-neuropilin 1 (MAB5661, R&D Systems; 1:100), rabbit polyclonal anti-collagen type 4 (#AB756P, Millipore; 1:200) and rabbit polyclonal anti-GFP (#sc-8334, Santa Cruz; 1:200). Fluorophore-coupled secondary antibodies were purchased from Dianova (goat anti-rabbit, #111-065-003) and Life Technologies (goat anti-rabbit and goat anti-rat, #A-11008 and #A-21434) and used at 1:200 or 1:250 dilution. Non-fluorescent staining was performed using kits from Vector Laboratories [Mouse-on-Mouse peroxidase kit, Vectastain ABC peroxidase kit (rabbit IgG), DAB substrate kit].

Explant cultures
For live cell imaging of GFP-labeled NDs, posterior trunks of E9.5 embryos were isolated and cultured with their flanks down on Transwell filters at 37°C in an atmosphere of 5% CO_2 for 18 h as previously described (Airik et al., 2010). GFP epifluorescence of NDs was documented hourly for the entire culture period.

Cellular assays
Apoptotic cells on 5 μm sections were detected by TUNEL assay, modifying genomic DNA via terminal deoxynucleotidyl transferase using the ApopTag Plus Fluorescein In Situ Apoptosis Detection Kit (Chemicon). All sections were counterstained with DAPI to visualize the nuclei.

In situ hybridization analysis
Whole-mount *in situ* hybridization was performed following a standard procedure with digoxigenin-labeled antisense riboprobes (Wilkinson and Nieto, 1993). Stained specimens were transferred to 80% glycerol prior to documentation. RNA *in situ* hybridization on 10 μm paraffin sections was essentially as previously described (Moorman et al., 2001). For each marker at least four independent specimens were analyzed.

Image analysis
Whole-mount specimens were photographed on a Leica M420 microscope with a Fujix HC-300Z digital camera, and sections on a Leica DM5000B with a Leica DFC300FX digital camera. GFP epifluorescence in living tissues was documented with a Leica DMI 6000 microscope, and the images and movies were processed with Leica Application Suite Advanced Fluorescence software (version 2.3.0). Confocal images were taken on a Leica Inverted-2 with TCS SP2 scan head. Images for figures were processed in Adobe Photoshop CS3.

Author contributions
A.-C.W., R.A. and A.K. initiated the project; A.-C.W., R.A., T.B., F.G., A.F., M.-O.T., C.R. and A.K. designed and performed the experiments; F.C. and R.H.A. provided mice; A.-C.W., M.-O.T., F.C., R.H.A. and A.K. wrote and/or edited the paper.

Supplementary material
Supplementary material available online at
http://dev.biologists.org/lookup/suppl/doi:10.1242/dev.113928/-/DC1

References

Airik, R. and Kispert, A. (2007). Down the tube of obstructive nephropathies: the importance of tissue interactions during ureter development. *Kidney Int.* **72**, 1459-1467.

Airik, R., Bussen, M., Singh, M. K., Petry, M. and Kispert, A. (2006). Tbx18 regulates the development of the ureteral mesenchyme. *J. Clin. Invest.* **116**, 663-674.

Airik, R., Trowe, M.-O., Foik, A., Farin, H. F., Petry, M., Schuster-Gossler, K., Schweizer, M., Scherer, G., Kist, R. and Kispert, A. (2010). Hydroureteronephrosis due to loss of Sox9-regulated smooth muscle cell differentiation of the ureteric mesenchyme. *Hum. Mol. Genet.* **19**, 4918-4929.

Batourina, E., Choi, C., Paragas, N., Bello, N., Hensle, T., Costantini, F. D., Schuchardt, A., Bacallao, R. L. and Mendelsohn, C. L. (2002). Distal ureter morphogenesis depends on epithelial cell remodeling mediated by vitamin A and Ret. *Nat. Genet.* **32**, 109-115.

Batourina, E., Tsai, S., Lambert, S., Sprenkle, P., Viana, R., Dutta, S., Hensle, T., Wang, F., Niederreither, K., McMahon, A. P. et al. (2005). Apoptosis induced by vitamin A signaling is crucial for connecting the ureters to the bladder. *Nat. Genet.* **37**, 1082-1089.

Bohnenpoll, T., Bettenhausen, E., Weiss, A.-C., Foik, A. B., Trowe, M.-O., Blank, P., Airik, R. and Kispert, A. (2013). Tbx18 expression demarcates multipotent precursor populations in the developing urogenital system but is exclusively required within the ureteric mesenchymal lineage to suppress a renal stromal fate. *Dev. Biol.* **380**, 25-36.

Bonanomi, D., Chivatakarn, O., Bai, G., Abdesselem, H., Lettieri, K., Marquardt, T., Pierchala, B. A. and Pfaff, S. L. (2012). Ret is a multifunctional coreceptor that integrates diffusible- and contact-axon guidance signals. *Cell* **148**, 568-582.

Chia, I., Grote, D., Marcotte, M., Batourina, E., Mendelsohn, C. and Bouchard, M. (2011). Nephric duct insertion is a crucial step in urinary tract maturation that is regulated by a Gata3-Raldh2-Ret molecular network in mice. *Development* **138**, 2089-2097.

Christoffels, V. M., Mommersteeg, M. T., Trowe, M.-O., Prall, O. W. J., de Gier-de Vries, C., Soufan, A. T., Bussen, M., Schuster-Gossler, K., Harvey, R. P., Moorman, A. F. M. et al. (2006). Formation of the venous pole of the heart from an Nkx2-5-negative precursor population requires Tbx18. *Circ. Res.* **98**, 1555-1563.

Costantini, F. and Shakya, R. (2006). GDNF/Ret signaling and the development of the kidney. *Bioessays* **28**, 117-127.

Dravis, C., Yokoyama, N., Chumley, M. J., Cowan, C. A., Silvany, R. E., Shay, J., Baker, L. A. and Henkemeyer, M. (2004). Bidirectional signaling mediated by ephrin-B2 and EphB2 controls urorectal development. *Dev. Biol.* **271**, 272-290.

Drawbridge, J., Meighan, C. M. and Mitchell, E. A. (2000). GDNF and GFRalpha-1 are components of the axolotl pronephric duct guidance system. *Dev. Biol.* **228**, 116-124.

Dufour, A., Seibt, J., Passante, L., Depaepe, V., Ciossek, T., Frisén, J., Kullander, K., Flanagan, J. G., Polleux, F. and Vanderhaeghen, P. (2003). Area specificity and topography of thalamocortical projections are controlled by ephrin/Eph genes. *Neuron* **39**, 453-465.

Gale, N. W., Holland, S. J., Valenzuela, D. M., Flenniken, A., Pan, L., Ryan, T. E., Henkemeyer, M., Strebhardt, K., Hirai, H., Wilkinson, D. G. et al. (1996). Eph receptors and ligands comprise two major specificity subclasses and are reciprocally compartmentalized during embryogenesis. *Neuron* **17**, 9-19.

Georgakopoulos, A., Xu, J., Xu, C., Mauger, G., Barthet, G. and Robakis, N. K. (2011). Presenilin1/gamma-secretase promotes the EphB2-induced phosphorylation of ephrinB2 by regulating phosphoprotein associated with glycosphingolipid-enriched microdomains/Csk binding protein. *FASEB J.* **25**, 3594-3604.

Grunwald, I. C., Korte, M., Adelmann, G., Plueck, A., Kullander, K., Adams, R. H., Frotscher, M., Bonhoeffer, T. and Klein, R. (2004). Hippocampal plasticity requires postsynaptic ephrinBs. *Nat. Neurosci.* **7**, 33-40.

Hoshi, M., Batourina, E., Mendelsohn, C. and Jain, S. (2012). Novel mechanisms of early upper and lower urinary tract patterning regulated by RetY1015 docking tyrosine in mice. *Development* **139**, 2405-2415.

Ingham, P. W. and McMahon, A. P. (2001). Hedgehog signaling in animal development: paradigms and principles. *Genes Dev.* **15**, 3059-3087.

Kao, T.-J., Law, C. and Kania, A. (2012). Eph and ephrin signaling: lessons learned from spinal motor neurons. *Semin. Cell Dev. Biol.* **23**, 83-91.

Kerecuk, L., Schreuder, M. F. and Woolf, A. S. (2008). Renal tract malformations: perspectives for nephrologists. *Nat. Clin. Pract. Nephrol.* **4**, 312-325.

Klein, R. (2012). Eph/ephrin signalling during development. *Development* **139**, 4105-4109.

Kramer, E. R., Knott, L., Su, F., Dessaud, E., Krull, C. E., Helmbacher, F. and Klein, R. (2006). Cooperation between GDNF/Ret and ephrinA/EphA4 signals for motor-axon pathway selection in the limb. *Neuron* **50**, 35-47.

Kullander, K. and Klein, R. (2002). Mechanisms and functions of Eph and ephrin signalling. *Nat. Rev. Mol. Cell Biol.* **3**, 475-486.

Kullander, K., Mather, N. K., Diella, F., Dottori, M., Boyd, A. W. and Klein, R. (2001). Kinase-dependent and kinase-independent functions of EphA4 receptors in major axon tract formation in vivo. *Neuron* **29**, 73-84.

Kuschert, S., Rowitch, D. H., Haenig, B., McMahon, A. P. and Kispert, A. (2001). Characterization of Pax-2 regulatory sequences that direct transgene expression in the Wolffian duct and its derivatives. *Dev. Biol.* **229**, 128-140.

Mackie, G. G. and Stephens, F. D. (1975). Duplex kidneys: a correlation of renal dysplasia with position of the ureteral orifice. *J. Urol.* **114**, 274-280.

Matt, N., Ghyselinck, N. B., Wendling, O., Chambon, P. and Mark, M. (2003). Retinoic acid-induced developmental defects are mediated by RARbeta/RXR heterodimers in the pharyngeal endoderm. *Development* **130**, 2083-2093.

Mendelsohn, C. (2009). Using mouse models to understand normal and abnormal urogenital tract development. *Organogenesis* **5**, 32-40.

Moorman, A. F. M., Houweling, A. C., de Boer, P. A. J. and Christoffels, V. M. (2001). Sensitive nonradioactive detection of mRNA in tissue sections: novel application of the whole-mount in situ hybridization protocol. *J. Histochem. Cytochem.* **49**, 1-8.

Morris, A. R., Drawbridge, J. and Steinberg, M. S. (2003). Axolotl pronephric duct migration requires an epidermally derived, laminin 1-containing extracellular matrix and the integrin receptor alpha6beta1. *Development* **130**, 5601-5608.

Muzumdar, M. D., Tasic, B., Miyamichi, K., Li, L. and Luo, L. (2007). A global double-fluorescent Cre reporter mouse. *Genesis* **45**, 593-605.

Nakai, H., Asanuma, H., Shishido, S., Kitahara, S. and Yasuda, K. (2003). Changing concepts in urological management of the congenital anomalies of kidney and urinary tract, CAKUT. *Pediatr. Int.* **45**, 634-641.

NAPRTCS (2007). *North American Pediatric Renal Trials and Collaborative Studies.* http://www.emmes.com/study/ped/annlrept/annlrept2007.pdf.

Obara-Ishihara, T., Kuhlman, J., Niswander, L. and Herzlinger, D. (1999). The surface ectoderm is essential for nephric duct formation in intermediate mesoderm. *Development* **126**, 1103-1108.

Ogawa, K., Wada, H., Okada, N., Harada, I., Nakajima, T., Pasquale, E. B. and Tsuyama, S. (2006). EphB2 and ephrin-B1 expressed in the adult kidney regulate the cytoarchitecture of medullary tubule cells through Rho family GTPases. *J. Cell Sci.* **119**, 559-570.

Palmer, A., Zimmer, M., Erdmann, K. S., Eulenburg, V., Porthin, A., Heumann, R., Deutsch, U. and Klein, R. (2002). EphrinB phosphorylation and reverse signaling: regulation by Src kinases and PTP-BL phosphatase. *Mol. Cell* **9**, 725-737.

Pedersen, A., Skjong, C. and Shawlot, W. (2005). Lim1 is required for nephric duct extension and ureteric bud morphogenesis. *Dev. Biol.* **288**, 571-581.

Pitulescu, M. E. and Adams, R. H. (2010). Eph/ephrin molecules–a hub for signaling and endocytosis. *Genes Dev.* **24**, 2480-2492.

Sallstrom, J., Peuckert, C., Gao, X., Larsson, E., Nilsson, A., Jensen, B. L., Onozato, M. L., Persson, A. E. G., Kullander, K. and Carlstrom, M. (2013). Impaired EphA4 signaling leads to congenital hydronephrosis, renal injury and hypertension. *Am. J. Physiol. Renal Physiol.* **305**, F71-F79.

Sebolt-Leopold, J. S. and Herrera, R. (2004). Targeting the mitogen-activated protein kinase cascade to treat cancer. *Nat. Rev. Cancer* **4**, 937-947.

Soufan, A. T., Ruijter, J. M., van den Hoff, M. J., de Boer, P. A., Hagoort, J. and Moorman, A. F. (2003). Three-dimensional reconstruction of gene expression patterns during cardiac development. *Physiol. Genomics* **13**, 187-195.

Srinivas, S., Goldberg, M. R., Watanabe, T., D'Agati, V., Al-Awqati, Q. and Costantini, F. (1999). Expression of green fluorescent protein in the ureteric bud of transgenic mice: a new tool for the analysis of ureteric bud morphogenesis. *Dev. Genet.* **24**, 241-251.

Treanor, J. J. S., Goodman, L., de Sauvage, F., Stone, D. M., Poulsen, K. T., Beck, C. D., Gray, C., Armanini, M. P., Pollock, R. A., Hefti, F. et al. (1996). Characterization of a multicomponent receptor for GDNF. *Nature* **382**, 80-83.

Trowe, M.-O., Maier, H., Petry, M., Schweizer, M., Schuster-Gossler, K. and Kispert, A. (2011). Impaired stria vascularis integrity upon loss of E-cadherin in basal cells. *Dev. Biol.* **359**, 95-107.

Tsou, H. C., Si, S. P., Lee, X., González-Serva, A. and Peacocke, M. (1994). A beta 2RARE-LacZ transgene identifies retinoic acid-mediated transcriptional activation in distinct cutaneous sites. *Exp. Cell Res.* **214**, 27-34.

Uetani, N. and Bouchard, M. (2009). Plumbing in the embryo: developmental defects of the urinary tracts. *Clin. Genet.* **75**, 307-317.

DEVELOPMENT

Uetani, N., Bertozzi, K., Chagnon, M. J., Hendriks, W., Tremblay, M. L. and Bouchard, M. (2009). Maturation of ureter-bladder connection in mice is controlled by LAR family receptor protein tyrosine phosphatases. *J. Clin. Invest.* **119**, 924-935.

Watanabe, T., Sato, Y., Saito, D., Tadokoro, R. and Takahashi, Y. (2009). EphrinB2 coordinates the formation of a morphological boundary and cell epithelialization during somite segmentation. *Proc. Natl. Acad. Sci. USA* **106**, 7467-7472.

Weber, S. (2012). Novel genetic aspects of congenital anomalies of kidney and urinary tract. *Curr. Opin. Pediatr.* **24**, 212-218.

Wilkinson, D. G. and Nieto, M. A. (1993). Detection of messenger RNA by in situ hybridization to tissue sections and whole mounts. *Methods Enzymol.* **225**, 361-373.

Woolf, A. S. and Davies, J. A. (2013). Cell biology of ureter development. *J. Am. Soc. Nephrol.* **24**, 19-25.

Wu, H.-C., Chang, C.-H., Peng, H.-Y., Chen, G.-D., Lai, C.-Y., Hsieh, M.-C. and Lin, T.-B. (2011). EphrinB2 induces pelvic-urethra reflex potentiation via Src kinase-dependent tyrosine phosphorylation of NR2B. *Am. J. Physiol. Renal Physiol.* **300**, F403-F411.

DEVELOPMENT